doi: 10.56761/EFRE2022.S1-P-049004

Simulation of a wide-aperture electron accelerator based on ion-electron emission in repetitively pulsed mode

A.A. Grishkov[*], *M.S. Vorobyov, S.Yu. Doroshkevich, V.A. Shklyaev*

Institute of High Current Electronics SB RAS, Tomsk, Russia
[*]*grishkov@to.hcei.tsc.ru*

Abstract. The paper proposes numerical and analytical approaches to modeling the generation of an electron beam in a repetitively pulsed regime of a wide-aperture electron accelerator based on secondary ion-electron emission with a plasma emitter. Some operating modes of the accelerator are simulated using known numerical codes and the developed approach. Qualitatively, the obtained experimental results are explained, which are in good agreement with the developed modeling approach.

Keywords: ion-electron emission, wide-aperture electron beam accelerator, beam extraction to the atmosphere, pulse mode, computer simulation.

1. Introduction

Currently, there is a diverse set of electron accelerators for a wide variety of scientific and technological problems. Simultaneous irradiation of large surfaces and volumes is a popular method of exposure in radiation technology, in ionization installations of gas lasers, in the creation of new materials, in medicine, and in other laboratory and applied problems [1–7].

A special position in this list is occupied by electron accelerators based on a non-self-sustained high-voltage glow discharge, which generate electron beams due to ion-electron emission when the cathode is bombarded with ions extracted from the auxiliary discharge plasma. Such accelerators favorably differ in relative simplicity of design and high service life of the main elements. However, the existing advantages of this type of accelerators are compensated by the high coupling of control parameters, which complicates their tuning and operation. In addition, accelerators of this type have a relatively low average coefficient of electron beam extraction into the atmosphere in a continuous mode of operation, which significantly limits the range of their application.

Recently, the use of a modern element base has made it possible to create discharge power supplies with a transition from the continuous mode of generating an auxiliary discharge to a pulsed mode with a pulse repetition rate at the level of a few to tens of kHz [8]. This allows more flexible adjustment of the discharge parameters, keeping the average value of its current, but changing its amplitude with a corresponding change in the duty cycle of the pulses. This approach made it possible to increase the current output coefficient, which is equal to the ratio of the beam current in the atmosphere to the current in the accelerating gap, from 0.25 in the continuous mode of operation to more than 0.5 in the repetitively pulsed mode of operation [9].

Due to the complex nature of the dependence of the current output coefficient on the control parameters, the high potential inherent in the transition from the continuous operation of the accelerator to the repetitively pulsed operation is difficult to study experimentally. Therefore, it seems logical to use modern numerical methods to develop in this direction.

However, this task is not easy either. Adaptation of existing numerical models and software for modeling the repetitively pulsed operation of an accelerator of this type is a relatively new task, since such models have not been developed in a comprehensive manner so far. This is due to the fact that there is no such software or program codes that would allow you to immediately simulate all the elements of the accelerator in a repetitively pulsed mode. And even if such software were available, the processing power requirements would be excessive. Therefore, from the point of view of modeling, it is logical to divide this problem into its constituent parts and study them separately by “sewing” solutions at the boundaries.

To study the formation and transport of charged particle beams in vacuum and gas, a narrow set of numerical methods and software codes is usually used. The problem is that for the accelerator under study, “classical” approaches will often be mutually exclusive for modeling individual elements of this accelerator. This means that if we use the PIC method together with the Monte Carlo method to simulate, for example, particle dynamics, then they describe beam transport, particle scattering and ionization well, but have a number of obvious weaknesses in the description of plasma. Simulation of PIC plasma is a separate complex problem, which we will not touch upon in this work.

If we consider the problem of beam focusing, then a complex electronic optical system requires detailed 3D modeling, but full 3D modeling for the PIC method is, again, a huge computational burden. If we take some iterative methods for solving (the method of successive approximations, the upper relaxation method, the finite element method, the current tube method) for solving stationary problems, then the problem is that it is necessary to simulate two diodes at once. If for a high-voltage diode, for example, with a voltage of hundreds of kilovolts, a deviation of tens of volts per finite-difference grid cell is quite acceptable, then for an auxiliary discharge, the voltage of which is on the order of hundreds of volts, the maximum deviation should be much less. In this regard, modeling of this type of electron accelerators is an urgent and demanded task. And in order to solve this problem, let's start by analyzing the experimental results obtained so far, and apply the available approaches to modeling such systems to describe them.

2. Experimental setup

The design of the accelerator (Fig.1) includes two main areas: the area of generation of an auxiliary discharge to create an anode plasma and the area of the main non-self-sustained high-voltage glow discharge. The boundary between these areas is established by means of an anode grid, the configuration of holes in which repeats the configuration of the holes in the support grid of the outlet foil window. The role of the auxiliary discharge is performed by an independent glow discharge, in which the anode is two tungsten wires, and the cathode is the walls of the vacuum chamber. The working gas (helium) is injected into the auxiliary discharge region between the wire anodes. Ions are extracted from the auxiliary discharge through holes in the anode grid, accelerated in the main gap and bombard the high voltage cathode, which leads to ion-electron emission. As a result of this process, electrons are generated, which are accelerated in the high-voltage gap and, passing through the holes of the anode and reference grids, are released into the atmosphere through a thin metal foil. The accelerator makes it possible to generate a wide (450×650 mm) continuous electron beam and extract it into the atmosphere through an exit window covered with AlMg alloy foil 30 μm thick. Beam parameters: electron energy up to 150 keV, beam current up to 50 mA, current density 1–15 μA/cm^2, limited by an average beam power not exceeding 7 kW, working gas pressure (7–40)$\cdot 10^{-3}$ Torr.

The experimental measurements and their features were described in more detail earlier [9–11]. From the experimental results obtained earlier, we are interested in the following point. Fig.2 shows typical current oscillograms for the repetitively pulsed regime: operating frequency 10 kHz, duty cycle 20%, average discharge current I_d = 30 mA, pressure $p = 5.6\cdot 10^{-3}$ Torr.

The results of the experiments showed that, upon switching to high-frequency generation of the auxiliary discharge and the same accelerating voltage, it was noticed that during the discharge current pulse, the coefficient of beam current output to the atmosphere can reach 0.5. In this case, the beam current has a rise time of a few microseconds. The most important nuance is that during a pause in the generation of the auxiliary discharge current, the output coefficient tends to zero, since the beam current in the atmosphere also drops to zero, and the current in the accelerating gap has a lower decay rate and changes insignificantly during the pause

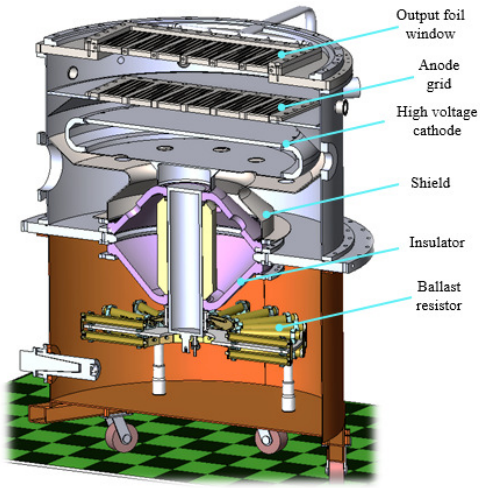

Fig.1. Design of simulated wide-aperture electron accelerator based on ion-electron emission in repetitively pulsed mode. Electron energy: up to 150 keV, beam current 1–40 mA, current density 1–15 μA/cm2.

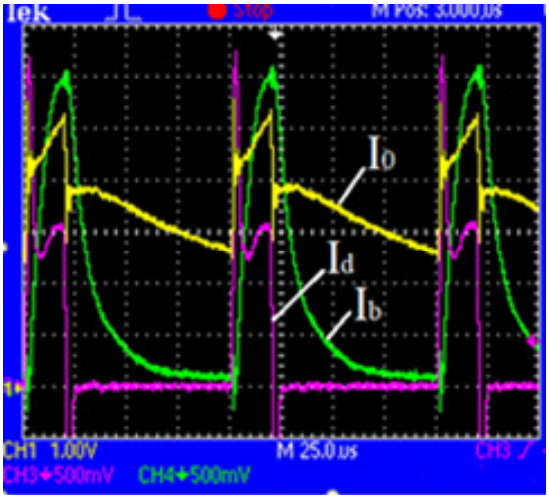

Fig.2. Oscillograms of currents (I_d = 30 mA, f = 10 kHz, p = 0.75 Pa): CH1 – current in accelerating gap I_0 (10 mA/div); CH3 – discharge current I_d (50 mA/div); CH4 – beam current I_b (5 mA/div).

Within the framework of this work, the task was set to develop a model explaining the absence of the beam current extracted into the atmosphere in the pause in the presence of a current in the main gap of the order of magnitude of the same amplitude as in the pulse. For this, several software products and approaches to accelerator modeling were used.

3. Theory and simulation

The area of generation of the auxiliary discharge for creating the anode plasma has a cylindrical shape with a diameter of 1070 mm and the height of 145 mm. Taking into account the dimensions of the anode grid (450×650 mm) and its geometric transparency (68%), it is possible to estimate the value of the ion current for one grid hole. The anode grid contains 270 holes; the ratio of the surface area of the hollow cathode to the area from which ions are extracted is $S_{grid}/S_{cathode}$ = 0.1. For the auxiliary discharge voltage of the order of U = 450 V and the current in the main gap I_0 = 80 mA, we get the value of the ion current for one hole is equals $I = 3 \cdot 10^{-5}$ A.

Let's make a small digression to voice the validity of such an assessment. In fact, there is no reliable experimental information about the uniform distribution of the current density inside the hollow cathode and that part of it that falls into the region of the anode grating. Traces of individual cathode spots were found on the cathode surface, especially at a high voltage of the auxiliary discharge. In addition, in the continuous operating mode of the accelerator, instabilities and inhomogeneities are observed in the discharge glow, which obviously indicates a non-uniform current distribution inside the hollow cathode. However, no traces were found on the cathode surface that a significant part of the current is concentrated in some local area. Therefore, while there are no direct measurements of the current density that falls on the grid, we will assume that it is distributed uniformly over the entire surface of the hollow cathode.

Let us determine the position of the plasma boundary inside the hollow cathode. The position of the emission boundary can be estimated from the joint solution of the Bohm and Child-Langmuir equations [12]:

$$0.4en\left(\frac{2kT_e}{M_i}\right) = \frac{8\pi}{9}\varepsilon_0\sqrt{\frac{2e}{M_i}}\frac{U^{\frac{3}{2}}}{d_c^{\,2}}, \qquad (1)$$

where n – the plasma density, T_e – the electron temperature, k – the Boltzmann constant, e – the electron charge, M_i – the ion mass, ε_0 – the electrical constant, U – the voltage in layer, and d_c – the cathode sheath width. Substituting the experimentally measured concentrations (10^{13}–10^{14} m^{-3}) and temperatures (3–5 eV) into this expression, we obtain $d_c \approx 2$–4 cm, depending on the specified parameters. It would be reasonable to make a similar estimate for a bipolar diode as well, since in general there are electrons in the cathode layer:

$$I_{3/2} = \frac{4}{9}\varepsilon_0 \sqrt{\frac{2e}{M_i}} \frac{S_{split}}{d_c^{\,2}} U^{\frac{3}{2}}. \qquad (2)$$

Based on the lattice parameters, we estimate the area of one hole $S_{split} = 10^{-3}$ m^2. For a bipolar diode, we obtain approximately the same range of values $d_c \approx 2$–4 cm.

This estimate allows us to say that the problem can be reduced to the case of injection of ions onto the anode lattice with an energy equal to the plasma potential relative to the cathode.

Examples of such a configuration in the single slit approximation are shown in Fig.3 and Fig.4. The simulation was carried out using the KOBRA3-INP code [13]. We used the commercial version of the KOBRA3-INP program. This code is well known as a tool for 3D simulation of charged particle generation systems. To simulate the process of beam extraction from plasma, the program includes a self-consistent algorithm for calculating the plasma boundary.

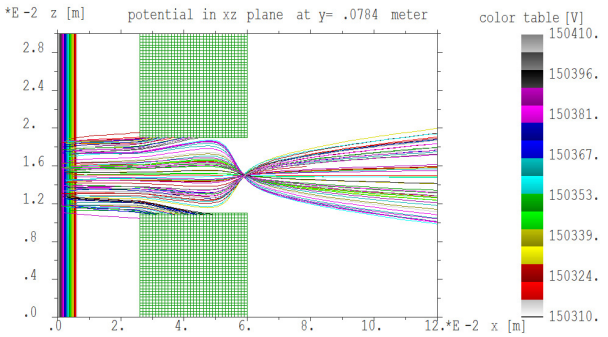

Fig.3. Simulation of a single slit by KOBRA3-INP code. Distribution of ion trajectories and potential. The area where the trajectories are specified (plasma boundary) is marked with color.

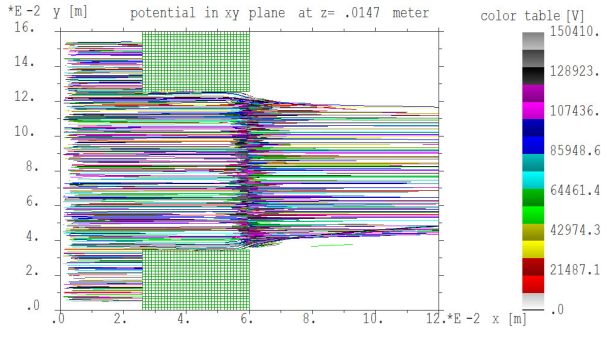

Fig.4. Simulation of a single slit by KOBRA3-INP code. Distribution of ion trajectories in transverse directions. The area where the trajectories are specified (plasma boundary) is located on left boundary.

At this point, it is important to note a few observations. Due to the shape of the slit (8×100 mm, with rounded edges), the nature of the distribution of trajectories in the longitudinal and transverse directions is different. A crossover is formed across the slit due to a strong electric field at the edges near the grid plane, which is turned towards the main gap. Along the gap, the nature of the trajectories is different. Due to the larger transverse size, the ion beam is only slightly compressed along the edges. From such a configuration of trajectories, it can be expected that, due to ion-electron emission, electrons will predominantly pass in the longitudinal direction and are partially absorbed by the grid in the transverse direction, since the wings of the ion beam distribution on the right boundary slightly extend beyond the slit area. A similar situation is observed for electrons, with the only difference that the slit optics endows the electron flow with a weak divergence, both in longitudinal and transverse projections.

At the same stage, the characteristic times of flight were estimated. The open-source code xoopic [14] and its commercial version OOPIC Pro were used to simulate particle dynamics. These software products are PIC + Monte Carlo codes, which are well known as tools for calculating the dynamics of particles, for solving various problems of the formation and transport of charged

particles in vacuum and gas. In most cases, OOPIC Pro code was used. This software modeled the emission and transport of electrons and ions, determined the losses of particle fluxes on the gratings, and calculated the parameters of the electron beam output into the atmosphere.

For the current computational geometry, for ions, the time of flight can be hundreds (up to 700) of nanoseconds. Moreover, most of the time (more than 500 ns) are spent on the transport of ions from the emission boundary to the region of the main non-self-sustaining high-voltage glow discharge. For electrons, the characteristic time of flight through the system (taking into account the intersection of the region of generation of the auxiliary discharge) is a few nanoseconds.

It should be noted that the determination of the nature of focusing of the ion and electron beams in a single slit (even of an arbitrary axisymmetric shape) is not a serious problem. Programs for trajectory analysis were available decades ago [15].

The simulation performed for a single slit confirms the estimates made earlier on the position of the plasma boundary. For the entire range of operating parameters with the auxiliary discharge turned on, the plasma boundary region is located inside the auxiliary discharge generation region.

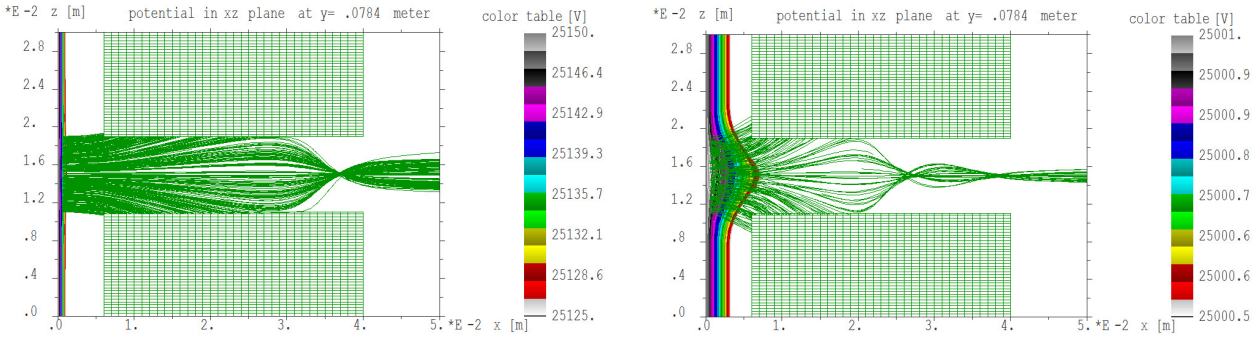

Fig.5. Simulation of the single slit by KOBRA3-INP. Distribution of ion trajectories (green) and potential map for plasma potential 150 V – (a), 10 V – (b).

Fig.5 shows two enlarged section of the computational domain with simulation parameters U_p = 10 V, 150 V, at a voltage in the main gap U_0 = 150 kV. It can be seen from the figures that the ion beam in both cases turns out to be focused, and for a plasma potential of 10 V, most of the trajectories are closed to the electrode. Let us analyze the dependence of the extracted ion current on the plasma potential.

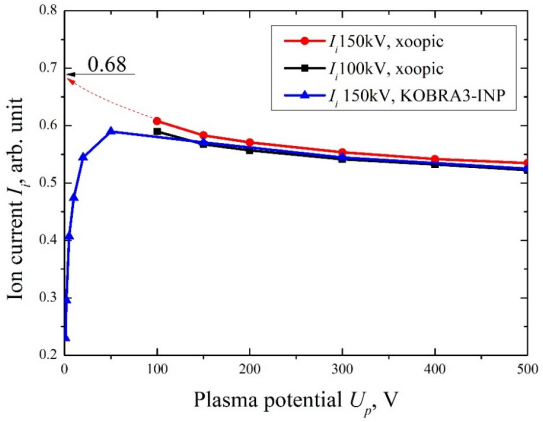

Fig.6. Dependence of the output current versus the plasma potential for the single slit from the KOBRA3-INP code and the five-slit array from the xoopic code.

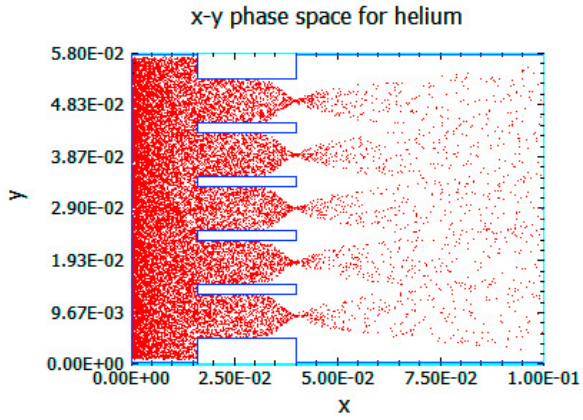

Fig.7. Simulation the five-slit array by the xoopic code. The location of the emission boundary was determined from KOBRA3-INP.

Fig.6 shows the dependences of the ion current for a single slit on the plasma potential for two different applied voltages in the high-voltage part. The same figure also shows the dependence of the ion current on the plasma potential for a five-slit array calculated by the OOPIC Pro code. Fig.7 shows the distribution of particles in the gap for this five-slit array. The position of the emission boundary for these simulations was determined from the results of the simulation by the KOBRA3-INP code. The position of the plasma boundary also agrees well with the results of our other work, where we investigated and simulated the auxiliary discharge of the accelerator under study [16]. The figures show the following. When the plasma potential decreases below 50 V, the passing ion current sharply decreases (Fig.6, blue curve), which begins to deposit on the anode grid. It is important to note that since in the xoopic and OOPIC Pro codes the plasma emission boundary was specified as flat rather than self-consistently calculated as in the KOBRA3-INP code, as the plasma potential decreased, the relative value of the ion current passing through the grating into the main gap tended to the coefficient lattice transparency. In Fig.6, this feature is shown with a red dotted line.

Thus, the conducted simulation shows that the system can be modeled separately for each element. There is no need to carry out a one-time calculation of the auxiliary discharge and the main gap for the ion beam. It is possible to separate these tasks and then stitch the solutions together to build a general model of the accelerator.

4. Electron beam extraction and ion beam in pause mode

An analysis of the beam current in the main gap shows that both during the auxiliary discharge and in the pause mode, the current in the main gap is at the same level in order of magnitude (100 mA and 60–80 mA, respectively, Fig.2.). Therefore, it is necessary to determine how and where this current is deposited and reproduced.

To solve this issue, we simulate an installation with an accelerating gap and an auxiliary discharge (Fig.8). Let there be a region of electron emission from the cathode, which is located opposite one of the slots in the anode grid and captures the adjacent edges of the grid. On a high-voltage cathode, we will set the boundary conditions for the emission of a background current of a small value uniformly distributed over the cathode surface. The applied voltage is 150 kV.

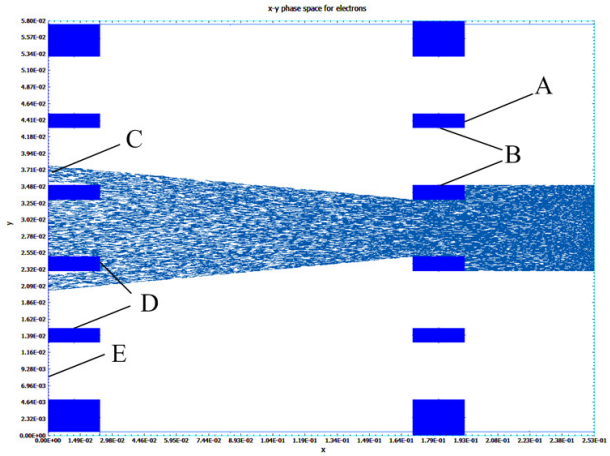

Fig.8. Distribution of electron trajectories from the local emission region on the cathode. U_0 = 150 kV. The letters ABCDE mark the zones of the computational domain into which the electron beam is deposited.

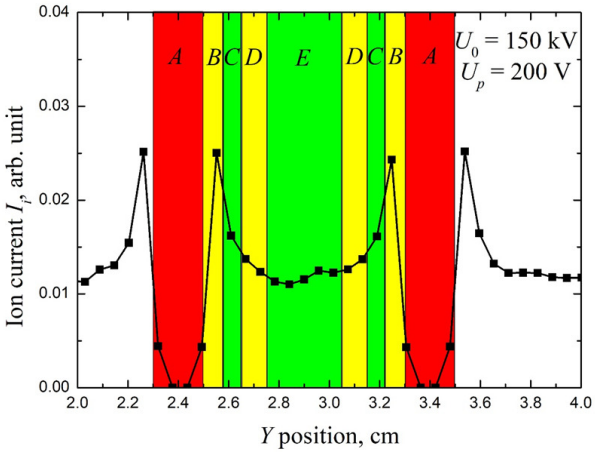

Fig.9. The distribution of the ion beam density in the cathode and the zones into which the electron beam emitted according to this distribution will be output. U_p = 200 V, U_0 = 150 kV. The letters ABCDE mark the zones of the computational domain from which the electron beam will be emitted.

The letters "A, B, C, D, E" will mark the zones of the computational domain into which the electron beam is deposited: "A" – the end face of the anode grid, "B" – the side surface of the anode grid, "C" – the adjacent slit of the support grid, "D" – the side and end surfaces of the support grid, "E" – hole in the support grid.

Trajectory analysis shows the following. The electrons start from the cathode and transport in a straight line towards the support grid. The simulation performed showed that with uniform emission from the cathode, about 50% of the electron current is deposited on the structural elements and does not enter to the output window. Part of the current is lost on the anode grid, part on the output. At the same time, it cannot be said that the edges of the output grid are in the region of the geometric shadow. Due to the curvature of the trajectories at the front and rear boundaries of the anode grid, part of the electron beam enters the region of the geometric shadow. In addition, part of the beam can also deposited on an adjacent slit in the output grid. This is another argument in favor of the fact that the "classical" simulation in the single-slit approximation does not suit us. It is important to note that much less electron current is deposited on the ends of the anode and output grid than on the side surface of the anode grid. About four times. Simply due to the fact that the area of the lateral surface of the anode grid is twelve times larger (the grid thickness is 24 mm). It may not be obvious from the drawings, as a different aspect ratio is used for visual display on the graph.

In real conditions, the electron emission is not uniformly distributed over the cathode. On Fig.9. The characteristic distribution of the ion current over the surface of a high-voltage cathode is shown for a plasma potential of 200 V and the applied voltage of 150 kV in the main gap. The same figure shows the zones from which the electron beam will be emitted and deposited to certain marked zones on various elements of the accelerator. It can be seen that most of the electron beam enters the output window (zone "E") and only a small part in zones "A", "B" and "D" hits various structural elements. This situation corresponds to the maximum extraction coefficients of the electron beam, which were recorded in experiments [11].

In the pause mode between pulses, the situation changes. As the plasma potential decreases (the auxiliary discharge is turned off), the fraction of the ion current into the region of the high-voltage gap drops rapidly (see Fig. 6, blue curve). This leads to the fact that the current of the electron beam, which is output to the atmosphere through the output window, also tends to zero. The simulation of this process is in good agreement with the results of previous experiments. But the question remains why in this mode the main gap retains the current, which remains in the order of magnitude of the same amplitude as in the pulse?

From the numerical simulation of the passage of the electron beam through the system (Fig.8), we determined the areas in the accelerator, which are the areas of leakage of the electron current. It is logical to assume that if an ion current is emitted from these regions or their vicinity, which will be closed in the regions on the cathode, from which the electron current is closed in the same regions, then this will create a closed current loop. Such a regime will lead to the fact that in the experiment a situation will be realized in which the current will remain in the main gap, while the current of the electron beam output into the atmosphere will tend to zero.

We can immediately exclude zones "A" and "D". Zone "A" due to the fact that simple current estimates (1)–(2) exclude such a possibility. If there were some emitting plasma on the edges of the grating, uniformly distributed over the grating, then currents of hundreds of amperes would have to be recorded in the system, which is not observed in the experiment. Zone "D" is also not suitable, because in the absence of an auxiliary discharge, the ions have nowhere to gain energy to reach the main gap. Remains area "B" - the side surface of the anode grid.

Fig.10 shows the distribution of ions in the computational domain when emission is specified from the side surface of the anode grating for the applied voltage of 150 kV. On Fig.11 the characteristic distribution of the ion current over the surface of the high-voltage cathode for these

conditions is shown. In the same figure, similarly to Fig.9, the zones into which the electron beam is deposited are indicated.

From the results of this series of calculations, the following picture emerges. At the moment, we cannot state with complete certainty what is the source of ions from the region of the side walls of the anode grid and its environs. This can be an auxiliary discharge plasma that penetrates into the grid channel, ionization of the residual gas or gas monolayers on the grid surface under the action of fast beam electrons, or some other processes. However, the simulations performed show that the presence of plasma in this region creates a closed (self-sustaining) circuit of trajectories and current, which can be reproduced and maintained during the pulse. A specially carried out series of calculations for various voltages applied to the main gap showed that this nature of the trajectories is preserved for any applied voltages. As an illustration of this thesis, Fig.12 shows the distribution of the ion current density from the side surface of the anode grid for two different applied voltages (100 kV and 150 kV). The figure shows a good agreement between the density distribution when the applied voltage changes by a factor of one and a half.

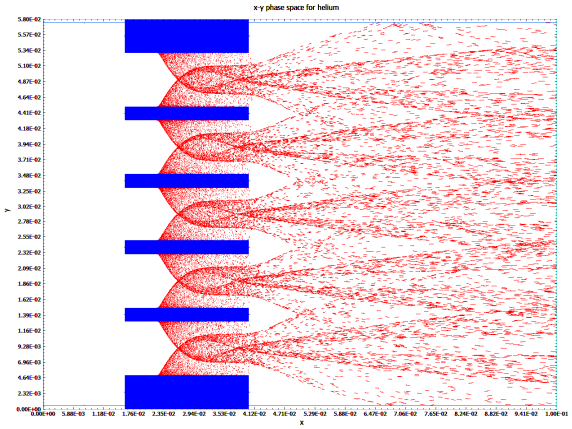

Fig.10. Distribution of ion trajectories emitted from the side surface of the slit of anode grid.

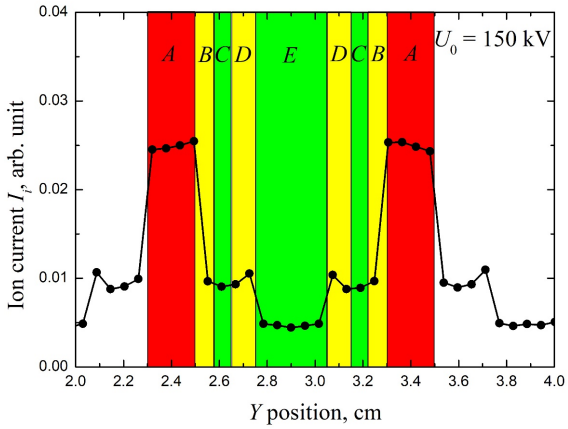

Fig.11. The distribution of the ion beam density on the cathode. The letters ABCDE mark the zones of the computational domain from which the electron beam will be emitted.

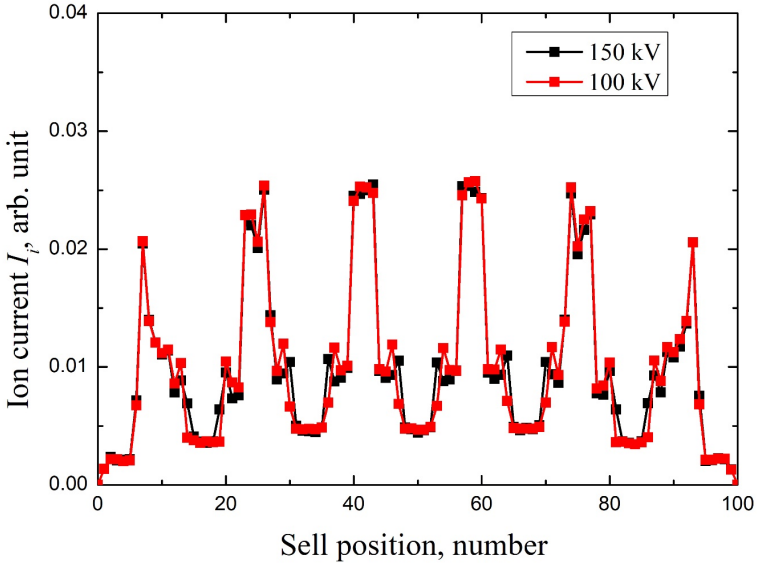

Fig.12. Density distribution on the cathode for ion current from the side surface of the slit of anode grid for different accelerating voltage.

The simulation performed showed that the magnitude and distribution of this current in a given configuration of the anode grid is practically independent of the parameters of the plasma potential and the accelerating voltage. This result perfectly explains the absence of the beam current extracted into the atmosphere in the pause in the presence of a current in the main gap of the order of magnitude of the same amplitude as in the pulse.

Modeling and analysis of oscillograms showed that in the repetitively pulsed mode of accelerator operation there is always this “parasitic” current addition in the main gap, which limits the coefficient of electron beam current output to the atmosphere. In connection with this result, further modeling work will be aimed at finding the optimal geometric parameters of the accelerating system and grid and physical conditions for optimizing the system for extracting ion and electron beams.

5. Conclusion

Thus, numerical simulations of the generation of an electron beam in a repetitively pulsed regime of a wide-aperture electron accelerator based on secondary ion-electron emission with a plasma emitter have been carried out in this work. The accelerator operation modes are modeled using known codes and the developed approach. Qualitatively, the obtained experimental results are explained, which are in good agreement with the developed modeling approach.

Modeling showed that the absence of an extracted electron beam in the pause mode in the presence of current in the main gap can be explained by the presence of closed trajectories to the side surface of the channel in the anode grid.

The ion current generated by these trajectories is constantly present in the main gap and causes a relatively low coefficient of electron beam extraction from vacuum to the atmosphere.

Acknowledgement

The work was carried out within the framework of the state assignment of the Ministry of Science and Higher Education of the Russian Federation on the topic FWRM-2021-0007, FWRM-2021-0014.

6. References

[1] Bugaev S.P., Kreyndel Yu.E., Schanin P.M., *Electron beams with a large cross section, (Electronniye puchki bol’shego secheniya (in Russian))*. (Moscow: Energoatomizdat, 1984).

[2] Sokovnin S.Yu., *Nanosecond electron accelerators and radiation technologies based on them (Nanosekundnie uskoriteli i radiatsionnie tehnologii na ih osnove (in Russian))*. (Yekaterinburg: UrO RAS. 2007).

[3] Pushkarev A.I., Novoselov Yu.N., Remnev G.E., *Chain processes in low-temperature plasma (Tsepnie protsessi v nizkotemperaturnoy plasme (in Russian))*. (Novosibirsk: Science, 2006).

[4] Rostov V.V., et al., *The Siberian Medical Journal*, (*Sibirskiy meditsinskiy jurnal*), **27**(1), 141, 2012;
url: https://elib.tomsk.ru/purl/1-8837/

[5] Novikov A.A., *Electron Sources of High-Voltage Glow Discharge with Anode Plasma (Istochniki electronov visokovoltnogo tleyushego razryada c anodnoy plazmoy (in Russian))*. (Moscow: Energoatomizdat, 1984).

[6] Pigache D., Fournier G., *J. Vac. Sci. Technol*., **12**(6), 1197, 1975; doi: 10.1116/1.568492

[7] Gurashvili V.A., et al., *Instruments and Experimental Techniques*, **63**(2), 227, 2020; doi: 10.1134/S0020441220030021

[8] Haijuan Mei, et al., *Surface & Coatings Technology*, **405**, 126514, 2020; doi: 10.1016/j.surfcoat.2020.126514

[9] Doroshkevich S.Yu., et al., *J. Phys.: Conf. Ser*., **2064**, 012116, 2021; doi: 10.1088/1742-6596/2064/1/012116
[10] Doroshkevich S., Levanisov V., Lopatin I., Vorobyov M., Torba M., Kovalsky S., Sulakshin S., *8th Int. Cong. on Energy Fluxes and Radiation Effects (EFRE) – 22st Int. Symp. on High-Current Electronics, 2–8 October, Tomsk, Book of abstract*, 22, 2022; url: https://efre2022.hcei.tsc.ru/files/abstracts/S1-O-031103.pdf
[11] Doroshkevich S., et al., *Proc. of 7th Int. Cong. on Energy Fluxes and Radiation Effects (EFRE) – 21st Int. Symp. on High-Current Electronics*, Tomsk, 42, 2020; doi: 10.1109/EFRE47760.2020
[12] Koval N.N., et al., *Emission Electronics (Emissonnaya electronica (in Russian))*. (Moscow: MSTU, 2009).
[13] Spädtke P., *KOBRA3-INP.* (Wiesbaden: Junkernstr, 1999).
[14] Verboncoeur J.P., et al., *Comput. Phys. Commun*., 87, 199, 1995; doi: 10.1016/0010-4655(94)00173-Y
[15] Brown I.G., (Ed.), *The Physics and Technology of Ion Sources. 2nd Edition. Chapter 5.* (Weinheim: Wiley-VCH, 2004);
[16] Grishkov A.A., Vorobyov M.S., Doroshkevich S.Yu., Shklyaev V.A., *Proc. of 8th Int. Cong. on Energy Fluxes and Radiation Effects, 2–8 October, Tomsk,* 2022; doi: 10.56761/EFRE2022.S1-P-049002